Journal of Toxicology and Environmental Health, Part A: Current Issues
Publication details, including instructions for authors and subscription information:
http://www.tandfonline.com/loi/uteh20

Toxicological Evaluation of Lung Responses After Intratracheal Exposure to Non-Dispersed Titanium Dioxide Nanorods

Jenny R. Roberts [a], Rebecca S. Chapman [a], Vijay R. Tirumala [b], Alamgir Karim [b], Bean T. Chen [a], Diane Schwegler-Berry [a], Aleksandr B. Stefaniak [c], Stephen S. Leonard [a] & James M. Antonini [a]

[a] Health Effects Laboratory Division, National Institute for Occupational Safety and Health, Morgantown, West Virginia, USA

[b] National Institute of Standards and Technology Polymers Division, Gaithersburg, Maryland, USA

[c] Division of Respiratory Disease Studies, National Institute for Occupational Safety and Health, Morgantown, West Virginia, USA

Available online: 02 May 2011

To cite this article: Jenny R. Roberts, Rebecca S. Chapman, Vijay R. Tirumala, Alamgir Karim, Bean T. Chen, Diane Schwegler-Berry, Aleksandr B. Stefaniak, Stephen S. Leonard & James M. Antonini (2011): Toxicological Evaluation of Lung Responses After Intratracheal Exposure to Non-Dispersed Titanium Dioxide Nanorods, Journal of Toxicology and Environmental Health, Part A: Current Issues, 74:12, 790-810

To link to this article: http://dx.doi.org/10.1080/15287394.2011.567954

Journal of Toxicology and Environmental Health, Part A, 74:790–810, 2011

ISSN: 1528-7394 print / 1087-2620 online
DOI: 10.1080/15287394.2011.567954

Taylor & Francis
Taylor & Francis Group

TOXICOLOGICAL EVALUATION OF LUNG RESPONSES AFTER INTRATRACHEAL EXPOSURE TO NON-DISPERSED TITANIUM DIOXIDE NANORODS

Jenny R. Roberts[1], Rebecca S. Chapman[1], Vijay R. Tirumala[2], Alamgir Karim[2], Bean T. Chen[1], Diane Schwegler-Berry[1], Aleksandr B. Stefaniak[3], Stephen S. Leonard[1], James M. Antonini[1]

[1]Health Effects Laboratory Division, National Institute for Occupational Safety and Health, Morgantown, West Virginia
[2]National Institute of Standards and Technology Polymers Division, Gaithersburg, Maryland
[3]Division of Respiratory Disease Studies, National Institute for Occupational Safety and Health, Morgantown, West Virginia, USA

Fine- and coarse-sized titanium dioxide (TiO_2) particles are considered to be relatively inert when inhaled. The goal of this study was to assess potential lung toxicity associated with well-characterized, non-dispersed rutile TiO_2 nanorods (10 × 40 nm). In vitro bioreactivity of TiO_2 nanorods was determined by electron spin resonance (ESR) to measure free radical production. To assess pulmonary effects in vivo, Sprague-Dawley rats were intratracheally instilled with saline, silica, or TiO_2 nanorods (10 μg, 100 μg, or 1 mg/rat). On d 1, 3, and 6 posttreatment, left lungs were preserved for microscopy and histopathology, and lung lavage was performed on right lungs. Additional rats were treated with saline or TiO_2 nanorods (100 μg or 1 mg/rat) on d 0, intratracheally inoculated with 5×10^5 *Listeria monocytogenes* on d 3, and bacterial clearance was assessed. ESR showed a significant concentration-dependent generation of hydroxyl radicals by TiO_2 nanorods in the presence and absence of macrophages; however, the hydroxyl radical signals from TiO_2 samples were low compared to silica. Rats exposed to 1 mg of TiO_2 nanorods had significantly elevated levels of lung injury, inflammation, and lavage fluid monocyte chemoattractant protein (MCP)-1 and macrophage inflammatory protein (MIP)-2 on d 1 and 3 that subsided by d 6, unlike the silica response that persisted. Immune cytokine secretion in the lung and bacterial clearance were not affected by preexposure to TiO_2 nanorods. To summarize, non-dispersed TiO_2 nanorods were found to induce radical formation and cellular oxidant production, and to generate transient and reversible pneumotoxic effects, and to not markedly alter pulmonary immune function.

Nanotechnology is a broad term that describes emerging technologies aimed at the development and application of materials in the nanometer size range, materials having a least one dimension of less than 100 nm (NIOSH 2009). It is estimated that within this decade, more than 2 million workers will be employed in the field of nanotechnology, and the global economic impact is expected to reach $1 trillion (Roco and Bainbridge 2003). In addition, the National Science and Technology Council (NSTC) identified inhalation as one of the primary routes of exposure to nanomaterials in occupational settings, including research and development, manufacturing, and processing/distribution (NSTC 2006).

Received 3 November 2010; accepted 16 December 2010.

The findings and conclusions in this report are those of the authors and do not necessarily represent the views of the National Institute for Occupational Safety and Health.

Current address for Vijay R. Tirumala is Cabot Corporation, Boston, MA 02210, USA; current address for Alamgir Karim is The University of Akron, Department of Polymer Engineering, Akron, OH 44325, USA.

Address correspondence to Jenny R. Roberts, PhD, Health Effects Laboratory Division, National Institute for Occupational Safety and Health (NIOSH), 1095 Willowdale Rd. (M/S 2015), Morgantown, WV 26505, USA. E-mail: jur6@cdc.gov

Therefore, there is a great need to understand the potential adverse health outcomes that may occur following nanoparticle exposure, and the mechanisms underlying these responses.

Animal studies showed that nanoparticles of identical composition and mass may be more toxic (Brown et al. 2001; Oberdoerster et al. 1992) and have increased deposition in the lungs (Brown et al. 2002; ICRP 1994; Jaques and Kim 2000; NIOSH 2007) when compared to their larger counterparts. In addition to particle size, other physicochemical properties were proposed to be considered in assessing the adverse effects of nanomaterials, such as agglomeration state, shape, crystal structure, chemical composition, surface area, surface chemistry, surface charge, and porosity (Warheit et al. 2007a). In previous years, coarse and fine titanium dioxide (TiO_2) was thought to be a low-toxicity particle (nuisance dust), suggesting that occupational exposure was not a significant hazard. With the emergence of nanotechnology, this assumption has been questioned with regard to nano-sized TiO_2 (Nel et al. 2006; Warheit et al. 2007b; Hamilton et al. 2009).

TiO_2 nanopowders are widely used in a variety of commercial applications that may result in occupational exposure, including additives in plastics, catalysts and catalyst supports, electrode materials for lithium batteries, inorganic membranes, pigments in paints, ink, polishing agents, fuel additives, ultraviolet (UV) protection, gas sensors, and photocatalytic and photochemical degradation of organic material and toxic chemicals (Dankovic et al. 2007). In addition to commercial use, TiO_2, particularly at the coarse and fine sizes, was used in pulmonary toxicity studies as a control or inert particle because it is insoluble, and relatively low in toxicity at doses below dust overload in the lungs (Warheit et al. 1997). Conflicting results from recent animal studies were observed in regard to the toxic potential of TiO_2 nanoparticles engineered for shape and size. Evidence suggests that exposure to TiO_2 nanomaterials may pose a health risk based on particle surface reactivity (Warheit et al. 2009) and shape (Watanabe et al. 2002; Hamilton et al. 2009). The contribution of size or surface area has been debated, with substantial effects noted in some studies (Sager et al. 2008) and minimal effect reported by others (Warheit et al. 2006). Shape is of importance because of the increased manufacture of fiber-shaped nanorods and nanowires that have advantages in applications of photocatalysis, photochromics, charge transfer, and sensing due to their unique structures (Chen and Mao 2006; Formo et al. 2008).

The goals of this study were to: (1) assess the pulmonary toxicity of a non-dispersed, well-characterized nanoparticle (TiO_2) of a composition that is considered to be relatively inert in the lung at fine and coarse particle sizes for comparison with future studies using a more dispersed form of the particle, (2) do so using the nanorod form of the material in order to establish a control particle for future experiments examining nanorods and nanowires of different composition, and (3) examine a range of doses to establish the lowest-observable-effect level (LOEL) or no-observable-effect level (NOEL), as well as a dose that may be expected to produce a significant inflammatory response in the lungs. To address these goals, a rutile TiO_2 nanorod was characterized for particle size, shape, and surface reactivity, and an in vivo animal model of pulmonary toxicity was employed that examined lung injury, inflammation, oxidative bioreactivity, and lung defense responses to bacterial lung infection after intratracheal instillation of the nanorods at three different doses.

METHODS

Particle Characterization

Rutile TiO_2 nanorods (10 nm $\times$ 40 nm) were purchased from Nanostructured and Amorphous Materials, Inc. (Houston, TX). See Table 1 for analyses of the TiO_2 nanorod sample. Surface area was measured using the dry powder form of the particle by the Brunauer, Emmett, and Teller (BET) method. Elemental composition was evaluated using inductively coupled plasma–atomic emission spectroscopy

TABLE 1. Reported and Measured Particle Characteristics

Physical properties	Specifications reported by manufacturer	Measurement method	Result
Primary geometric particle size	10 × 40 nm	FESEM/TEM	7.60 ± 1.4 × 35.9 ± 6.2 nm
Specific surface area	160 ± 30 m^2/g	BET method	160.34 m^2/g
Purity	TiO_2, rutile >98 % with SiO_2 coating (<5%)	ICP-AES	$TiO_2 \geq$ 99% weight
Agglomerate size in PBS after 30-s sonication	ND	DLS	500–2800 nm
Number of agglomerates/mg	ND	Mathematical Calculation	$1.45 \cdot 10^9$–$1.53 \cdot 10^{11}$

Note. FESEM = field emission scanning electron microscopy, TEM = transmission electron microscopy, BET =Brunauer, Emmett, and Teller (BET) method, ICP-AES = inductively coupled plasma–atomic emission spectroscopy, PBS = phosphate-buffered saline, DLS = dynamic light scattering, ND = not determined.

(ICP-AES). Field emission scanning electron microscopy (FESEM), dynamic light scattering (DLS), and small-angle x-ray scattering (SAXS) were employed to analyze size distribution and agglomeration in the vehicle, phosphate-buffered saline (PBS). Particle surface reactivity was evaluated using electron spin resonance (ESR).

Surface area. Surface area was measured by gas adsorption using a Quantachrome NOVA 220e surface area analyzer and ultra-high-purity nitrogen gas as the adsorbate (cross-sectional area of 16.2 $Å^2$). TiO_2 nanorods were loaded into a preweighed sample cell and outgassed under vacuum (0.013 torr) for 5 h at 200°C to remove moisture from the powder. Before analysis, the sample was cooled and weighed on an analytical balance. Surface area was measured using 7 adsorption points for relative pressures between 0.05 and 0.35 (ASTM 2002); results were normalized by dry powder mass to obtain specific surface area.

Elemental composition. TiO_2 nanorods were evaluated by ICP-AES, according to NIOSH method 7300 modified for microwave digestion (NIOSH 1996). The nanorods were weighed and analyzed for elemental metal content by weight using a Fisons Accuris ICP emission spectrometer (Fisons Instruments, Beverly, MA).

Dynamic light scattering (DLS). DLS measurements were performed at the National Institute for Standards and Technology (NIST). TiO_2 was diluted in PBS (0.2 mg/ml) and sonicated for 30 s prior to measurement. Measurements were performed at 25°C using a Brookhaven Instruments (Brookhaven, NY) BI-200SM laser light scattering setup equipped with a BI-9010AT autocorrelator. Scattering data were collected on the sample at a 90° angle relative to the incident light. The sample was measured for 30 s periodically over a period of 30 min to ensure reproducibility of the autocorrelation function. Data were analyzed using regularized non-linear least square fitting procedure (CONTIN) to allow for multimodal distribution of particle size.

Particle number per mass. Using particle (agglomerate) diameter measurements made with DLS and incorporating the bulk density reported by the manufacturer, the number of particles (agglomerates) in 1 mg of TiO_2 nanorods can be theoretically calculated using the following equation: Number of particles (agglomerates) in 1 mg/mass per particle (agglomerate) $= 1/[(\pi D^3/6) \cdot \rho \cdot 10^{-18}]$, where D is the agglomerate diameter, ρ is the bulk density, and 10^{-18} is the conversion factor for g/cm^3 to mg/nm^3.

Small-angle x-ray scattering (SAXS). SAXS measurements were performed at NIST using a custom-designed Rigaku-Molecular Metrology SAXS instrument that uses x-rays of 16 keV incident energy. Samples were prepared at 30 mg/ml and 3 mg/ml in PBS, and sonicated for 30 s prior to measurements. Samples were

measured at 25°C in air for 5 min each over a period of 3 h, to check for reproducibility. Scattered x-rays were collected onto a detector located at a distance of 2 m, which corresponds to a measured q-range of 0.01 $nm^{-1} < q < 2\ nm^{-1}$, where $q = (4\pi/\lambda)\sin(\theta)$ and 2θ is the angle over which scattering data are collected. The raw scattering data from each sample were azimuthally averaged and were presented without further corrections.

Field emission scanning electron microscopy (FESEM) and transmission electron microscopy (TEM). TiO_2 nanorods were suspended in PBS, diluted in deionized water, dried onto carbon planchets, and imaged using a Hitachi model S-4800 field emission scanning electron microscope between 5 and 20 kV. Primary particle size was measured from micrographs obtained by transmission electron microscopy (JEM-1220, JEOL Ltd).

Electron spin resonance (ESR). The generation of the hydroxyl radicals on the particle surface as an indicator of surface reactivity was evaluated by ESR using an EMX spectrometer (Bruker Instruments, Inc., Billerica, MA) and a flat cell assembly. This technique involved the addition-type reaction of a short-lived radical with a diamagnetic compound (spin trap) to form a relatively long-lived free radical product (the spin adduct), which can be observed by conventional ESR (Janzen and Blackburn 1968). For this study, hydroxyl radical was generated from a Fenton-like reaction system after TiO_2 (10 μg, 100 μg, or 1 mg) or silica (Min-U-Sil α-quartz, US Silica Co., Berkeley Springs, WV; positive control; 1 mg or 100 μg) with H_2O_2 [1 m*M*] was combined in the presence of 100 m*M* of the spin trap 5,5-dimethyl-1-pyrroline *N*-oxide (DMPO) and PBS to a final volume of 1 ml. Reactions were allowed to incubate 3 min at room temperature before measurement and then transferred to a flat cell for ESR measurement. Signal intensity of the spin adduct, which corresponds to the amount of a given radical species, was determined by integration of the characteristic wave form for that radical. The wave form was then measured and quantified.

Animals

Male Sprague-Dawley [Hla:(SD)CVF] rats (Hilltop Laboratories, Scottdale, PA) weighing 250–300 g, approximately 10 wk old, were used for all experiments in accordance with a protocol approved by the institute's Animal Care and Use Committee (ACUC). Animals were given a Teklad 2918 diet and tap water ad libitum, housed in a clean air and viral- and antigen-free room with restricted access in an Association for Assessment and Accreditation of Laboratory Animal Care International (AAALAC)-approved animal facility, and allowed to acclimate for 1 wk before use. The rats were monitored and found to be free of endogenous viral pathogens, parasites, mycoplasms, *Helicobacter*, and CAR *Bacillus*.

Free Radical Production by Primary Alveolar Macrophages (AM) In Vitro

Whole lung lavage was performed by washing the lungs of the naive rats with aliquots of PBS in order to obtain primary alveolar macrophages (AM). Briefly, rats were euthanized with an overdose of sodium pentobarbital (>100 mg/kg body weight; Sleepaway, Fort Dodge Animal Health, Wyeth, Madison, NJ), the trachea was cannulated, the chest cavity was opened, and lavage was performed on the lungs via the tracheal cannula. Five washes of 6 ml each of PBS were performed while massaging the chest cavity. The collected fluid was then centrifuged (10 min, 1200 × g) and the cell pellet was resuspended in 1 ml PBS. Cells were counted using a Coulter Multisizer II (Coulter Electronics, Hialeah, FL) to determine the total number of AM recovered from the lavage. ESR was then used to evaluate free radical production by primary AM treated with TiO_2 nanorods in vitro; 1×10^6 AM were suspended in PBS, stimulated for 5 min at 37°C with 10 μg, 100 μg, or 1 mg of TiO_2 or PBS ($n = 3$ per group) in the presence of DMPO (200 mM). Cells treated with 1 mg or 100 μg of silica served as a positive control. Generation of hydroxyl radicals by AM was quantified by ESR as described earlier.

In Vivo TiO_2 Exposure

A stock suspension of the TiO_2 nanorods or silica (positive control) was prepared in sterile PBS at a concentration of 10 mg/ml and sonicated for 30 s at 10 W. The stock suspension was then further diluted in PBS to concentrations of 3.33, 0.333, or 0.033 mg/ml. Rats weighing 300 g were anesthetized with an intraperitoneal injection of 0.6 ml of a 1% solution of sodium methohexital (Brevital, Eli Lilly, Indianapolis, IN), and intratracheal instillation (IT) was performed with a volume of 300 μl of the TiO_2 or silica solutions, which was equivalent to 10 μg, 100 μg, or 1 mg of TiO_2 or silica per rat, or with sterile PBS (saline, vehicle control), according to the method of Brain et al. (1976).

Calculations were made to estimate the dose equivalents in standard workers, defined as 31% sitting and 69% light exercise with a minute ventilation of 20 L, using the National Institute for Occupational Safety and Health (NIOSH) recommended exposure limit (REL) (NIOSH 2005) for both ultrafine (primary particle size) and fine (agglomerate size) TiO_2 for a standard work shift (an 8-h day or 480 min). The calculation for deposition efficiency was based on the average aggregate size. The deposition equation is as follows:

$$\begin{aligned}\text{Particle deposition in a 75 kg standard worker} &= (\text{minute ventilation}) \times (\text{TLV-TWA}) \\ &\times (\text{exposure time}) \times (\text{particle lung deposition efficiency})\end{aligned}$$

where TLV-TWA is threshold limit value, time-weighted average. For agglomerates, the deposition is primarily based on the aerodynamic behavior of the TiO_2 nanorod complex, rather than a single nanorod. From the particle characterization, the TiO_2 rods were found to form agglomerates with a number-based mean equivalent diameter ($D_{eq,agg}$) of 2.37 μm and a geometric standard deviation of 2.28. Using the bulk density of the nanorod reported by the manufacturer (0.1 g/cm^3) and assuming a shape factor of 1.15 (based on an aspect ratio of 4 or less), the corresponding mass-based aerodynamic diameter ($D_{ae,agg}$) is approximately 0.64 μm. For these agglomerates, the deposition efficiency in the pulmonary region of a standard worker is about 7.8% (ICRP 1994). The NIOSH recommended exposure limit (REL) for fine TiO_2 is 1.5 mg/m^3. Using these values:

$$\begin{aligned}\text{Particle deposition in the standard worker} &= (20{,}000\ \text{ml/min}) \times (10^{-6}\text{m}^3/\text{ml}) \\ &\times (1.5\ \text{mg/m}^3) \times (480\ \text{min/d}) \\ &\times (0.078) \\ &= 1.123\ \text{mg/d}\end{aligned}$$

$$\begin{aligned}\text{Normalizing for alveolar epithelial surface area of a 75-kg human and a 300-g rat (human} &= \sim 102.2\ \text{m}^2\text{; rat} = \sim 0.4\ \text{m}^2) \\ &= 1.123\ \text{mg/d} \times (0.4\text{m}^2/102.2\ \text{m}^2) \\ &= 0.0044\ \text{mg/d or } 4.4\ \mu\text{g/d}\end{aligned}$$

Applying this value to the doses administered to the rats in this study, a 10-μg dose is equivalent to approximately 2.3 work days, 100 μg is equivalent to approximately 23 work days, and 1 mg is equivalent to approximately 227 work days or, assuming a 5-day work week, 45.4 wk.

Alternately, if deposition is calculated based on the REL related to the primary particle size, the REL for ultrafine TiO_2 (0.1 mg/m^3) can be employed with the equations given earlier and the equivalent doses can be calculated. Using this value, the deposited mass in a standard worker in one work day would equal 0.075 mg/d. When normalized to alveolar surface area in the rat, this yields 0.293 μg/d. Therefore, using the ultrafine REL, a 10-μg dose in the rat is equivalent to 34 work days, a 100-μg dose is equivalent to 341 work days (68.2 wk), and a 1-mg dose is approximately 3410 work days (682 wk or about 13 years).

Lung Lavage Cell and Fluid Collection Postexposure

Whole lung lavage was performed by washing the lungs of the rats with aliquots of PBS in order to obtain pulmonary cells for morphological and functional analysis, and acellular lavage fluid was retained for analysis of indicators of tissue damage and cellular activity. Rats were euthanized with an overdose of sodium pentobarbital (>100 mg/kg body weight; Sleepaway, Fort Dodge Animal Health, Wyeth, Madison, NJ); the trachea was cannulated, the chest cavity was opened, the left lung was clamped off, and lavage was performed on the right lung via the tracheal cannula 1, 3, or 6 d post-IT. The acellular fraction of the first lavage was obtained by filling the right lung with 1 ml/100 g body weight of PBS, massaging for 30 s, withdrawing, and repeating the process one more time. This concentrated aliquot was withdrawn, retained, kept separately, and was designated as the first fraction of lavage fluid. The following aliquots were 6 ml in volume, instilled once with light massaging, withdrawn, and combined until a 30-ml volume was obtained. For each animal, both lavage fractions were centrifuged (10 min, 1200 × g), the cell pellets were combined and resuspended in 1 ml PBS, and the acellular fluid from the first fraction was retained for further analysis.

Histopathological Evaluation

The left lungs of two rats per group from the TiO_2 and saline groups per time point were fixed with 10% neutral buffered formalin by airway fixation at total lung capacity. The left lungs were embedded in paraffin, sectioned onto slides, and stained with hematoxylin and eosin (H&E). H&E-stained slides were qualitatively analyzed for indications of inflammation and injury by a certified veterinary pathologist at Charles River Laboratories (Wilmington, MA) who was blinded to the treatment groups. Indices of inflammation and injury were scored on scale of 0–5, where 0 = no observed effect, 1 = minimal response, 2 = mild response, 4 = moderate response, and 5 = severe response.

Analysis of Albumin and Lactate Dehydrogenase (LDH) Activity

The presence of albumin and lactate dcehydrogenase (LDH) activity in the lung lavage fluid of all treatment groups was measured to evaluate the loss of integrity of the alveolar–capillary barrier and general cytotoxicity, respectively. Measurements of both albumin and LDH activity in the acellular fluid were obtained using a Cobas Mira analyzer (Roche Diagnostic Systems, Montclair, NJ). Albumin was determined by spectrophotometric measurement of the reaction product of albumin with bromcresol green (628 nm) according to a method by Sigma Diagnostics (St. Louis, MO). LDH activity was quantified by detection of the oxidation of lactate coupled to the reduction of NAD^+ at a spectrophotometric setting of 340 nm.

Lung Lavage Cell Differentials and Particle Uptake by AM

Total lung lavage cells collected from rats treated with TiO_2 nanorods, silica, or PBS were counted using a Coulter Multisizer II (Coulter Electronics, Hialeah, FL). Cell differentials were performed to determine the total number of alveolar macrophages (AM), neutrophils, and lymphocytes. Briefly, 1×10^5 cells from each rat were spun down onto slides with a Cytospin 3 centrifuge (Shandon Life Sciences International, Cheshire, England) and labeled with Leukostat stain (Fisher Scientific, Pittsburgh, PA) to differentiate cell types. Two hundred cells per slide were counted, and the percentages of AM, neutrophils, and lymphocytes were multiplied by the total number of cells to calculate the total number of each cell type.

Particle uptake by AM recovered from treated rats at each dose and at each time point was evaluated using scanning electron microscopy (SEM) and transmission electron

microscopy (TEM). Particles in AM were verified to be TiO_2 nanorods using energy-dispersive x-ray (EDX) analysis at 20 kV.

Lung Lavage Fluid Cytokine Analysis

Cytokines and chemokines involved in inflammatory and immune responses were measured in the first fraction of lavage fluid of rats pretreated with TiO_2 nanorods, silica, or PBS using commercially available enzyme-linked immunosorbent assay (ELISA) kits (BioSource International Inc., Camarillo, CA). The following cytokines and chemokines were quantified: tumor necrosis factor-α (TNF-α), interleukin (IL)-2, IL-4, IL-6, IL-10, IL-12p70, interferon-γ (IFN-γ), monocyte chemotactic protein (MCP)-1, and macrophage inflammatory protein (MIP)-2.

Lung Infectivity Model

Lung immune response to infection after exposure to TiO_2 nanorods was evaluated using a well-established bacterial infectivity model (Antonini et al. 2002; Cohen et al. 2001; Roberts et al. 2007; Van Loveren et al. 1988). In this model, bacteria is administered IT 3 d after particle exposure, at which point any potential confounding effects due to the method of particle administration have subsided and alterations in lung immune responses (bacterial clearance) in the lung can be directly attributed to adverse effects of the particle itself on the lung.

Intratracheal bacteria inoculation. *Listeria monocytogenes* was cultured overnight in brain–heart infusion broth (Difco Laboratories, Detroit, MI) at 37°C in a shaking incubator. Following incubation, the bacterial concentration was determined spectrophotometrically at an optical density of 600 nm. The sample was diluted to the concentration of 5×10^5 *L. monocytogenes* in 500 μl of sterile PBS and administered IT to the rats 3 d after instillation of TiO_2 nanorods (100 μg or 1 mg) or saline ($n = 6$ per group per time point).

Morbidity/pulmonary clearance of L. monocytogenes. Morbidity and pulmonary clearance were monitored in animals pretreated with TiO_2 nanorods or saline. Animal weights were monitored over the course of the treatment period as an indicator of morbidity. Rats were euthanized with an overdose of sodium pentobarbital (>100 mg/kg body weight; Sleepaway, Fort Dodge Animal Health, Wyeth, Madison, NJ), and at d 6, 8, and 10 (corresponding to d 3, 5, and 7 postinfection), and the left lung was removed from all the rats in each treatment group. The excised tissues were suspended in 10 ml sterile water, homogenized using a PowerGen 700 homogenizer (Fisher Scientific, Pittsburgh, PA), and cultured quantitatively on brain–heart infusion agar plates (Becton Dickinson and Co., Cockeysville, MD). The number of colony-forming units (CFUs) was counted after an overnight incubation at 37°C.

Statistical Analysis

Results are expressed as means ± standard error of measurement (SE). Statistical analyses were carried out with the SigmaStat 3.1 statistical program (Chicago). The significance of the interaction among different treatment groups for the different parameters at each time point was assessed using analysis of variance (ANOVA). The significance of difference between individual groups was analyzed using the Holm–Sidak method with the criterion of significance set at $p < .05$.

RESULTS

TiO_2 nanorods were analyzed for composition and were found to be >99% TiO_2 by weight. The nanorods acquire an amorphous SiO_2 coating during manufacturing. In this sample, that coating would be <1% weight yielding less than 10, 1, or 0.1 μg of SiO_2 in the 1 mg, 100 μg, or 10 μg TiO_2 nanorod treatment, respectively. At this concentration, the SiO_2 coating is not likely to attribute overtly to toxicity of the particle (Merget et al. 2002). In

the dry powder form, the manufacturer indicated that the TiO_2 nanorods had a primary geometric particle size of 10 nm × 40 nm (Table 1). Measurements of the TiO_2 nanorods made by our group using FESEM/TEM gave slightly smaller results with physical dimensions of 7.6 nm × 35.9 nm. TiO_2 nanorods were suspended in PBS for treatment of cells and animals. DLS measurements showed the range in agglomerate size to be approximately 500–2800 nm (Table 1) with an average $D_{eq\ agg}$ of 2370 nm. The distribution was bimodal, and when the suspension was allowed to settle over time there was a small fraction that still remained in suspension with a smaller diameter range of 450–1300 nm (data not shown; however, this was not representative of the bulk sample). Using DLS measurements and the bulk density range reported by the manufacture (0.06–0.1 g/cm^3), the range in agglomerate number in 1 mg of TiO_2 nanorods was calculated (Table 1). Using the equation described in the methods section, and assuming the largest agglomerate size (2800 nm) and the lowest bulk density (0.06 g/cm^3), the lowest number of agglomerates in 1 mg was calculated as follows:

$$\text{Number of agglomerates per 1 mg} = 1/[(\pi D^3/6) \cdot \rho \cdot 10^{-18}]$$

$$= 1/[(3.1416) \cdot (2800)^3 \cdot (0.06) \cdot (10^{-18})/6]$$

$$= 1.45 \times 10^9$$

Assuming the smallest agglomerate (500 nm) and the largest bulk density (0.1 g/cm^3), the highest number of agglomerates in 1 mg was calculated as follows:

$$\text{Number of agglomerates per 1 mg} = 1/[(\pi D^3/6) \cdot \rho \cdot 10^{-18}]$$

$$= 1/[(3.1416) \cdot (500)^3 \cdot (0.1) \cdot (10^{-18})/6]$$

$$= 1.53 \times 10^{11}$$

SAXS analysis of the 30 mg/ml suspension of TiO_2 nanorods in PBS showed that the primary particle aggregate was a cluster of 3–4 rods oriented along their length (Figure 1A). The high concentration was used for analysis as it remained in suspension over longer periods of time compared to the other concentrations. The analysis of the 3 mg/ml suspension, which corresponds to the 1-mg dose in the in vivo studies, was found to have a similar primary aggregate size and orientation; however, it settled out of suspension more rapidly over time. Figure 1B represents an example of how the primary nanorods aggregated together to form more complex clusters of particles that are representative of their structure in suspension with an average particle diameter in the fine size range. In agreement with the SAXS analysis, FESEM depicted the formation of small aggregates of TiO_2 nanorods after the particle suspensions were dried (Figure 2).

In analysis of the reactivity of the TiO_2 nanorods, ESR was performed to measure free radical production by TiO_2 nanorod samples in a cell-free suspension (Figure 3) and in the presence of AM collected from naive, untreated rats (Figure 4). There was a concentration-dependent production of the hydroxyl radical by the TiO_2 nanorods in suspension, with the 10 μg concentration showing no reactivity relative to control (Figure 3B). However, when compared to equivalent concentrations of silica, the TiO_2 nanorods were significantly less reactive in suspensions. Similar findings were observed when the TiO_2 nanorod suspensions were incubated in the presence of AMs (Figure 4). The highest dose of the TiO_2 nanorod suspensions induced a significant elevation in hydroxyl radical formation after AM treatment compared to control (Figure 4B). However, this increase was dramatically less when compared to the response generated by an equivalent concentration of silica, the positive control.

Histological analysis was performed on H&E-stained tissue sections to assess the potential pneumotoxic effect of TiO_2 nanorods after in vivo treatment (Figure 5). Rats treated with 10 μg TiO_2 showed minimal inflammation and granulocyte infiltration at 1 d

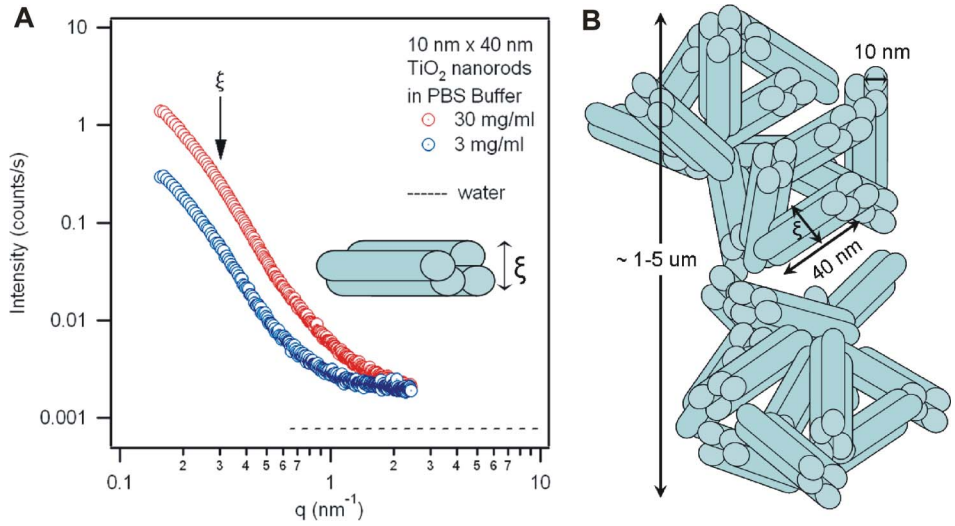

FIGURE 1. (A) SAXS analysis of a 30-mg/ml and a 3-mg/ml TiO_2 nanorod suspension in PBS (30 sec sonication) depicting the primary aggregate size and shape. Primary aggregate size was similar at both concentrations and consisted of three to four rods oriented along their length. Stability in suspension, the degree to which the particles remained suspended in the solution and did not precipitate, was found to decrease with decreasing concentration. (B) A representative schematic of how the primary aggregates agglomerate in suspension; ξ represents the average correlation length corresponding to the diameter of the primary aggregate (color figure available online).

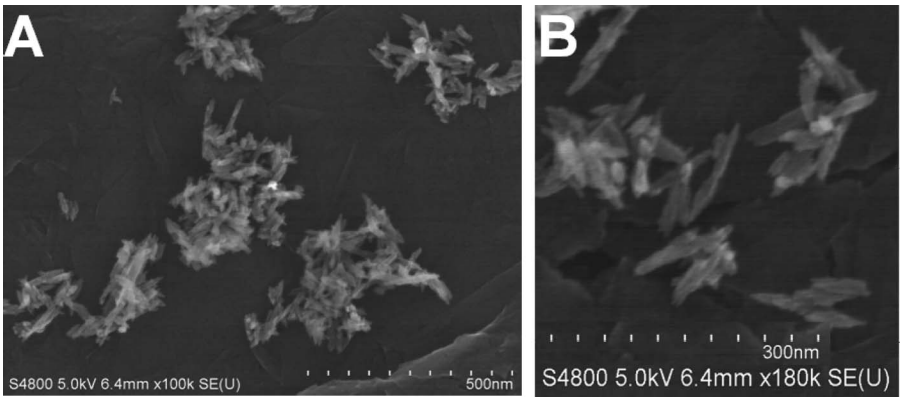

FIGURE 2. Field emission scanning electron micrographs (FESEM) of TiO_2 nanorods dried onto carbon planchets. FESEM images show small aggregates of nanorods reported to have a primary particle size of 10 nm x 40 nm. (A) Micron bar = 500 nm; subdivisions of bar = 50 nm. (B) Micron bar = 300 nm, subdivisions of bar = 30 nm.

postinstillation only with no other histological changes (data not shown). Rats exposed to 100 μg or 1 mg TiO_2 demonstrated mild inflammation, infiltration of granulocytes, and damage or alteration to epithelial cells at 1 d postinstillation (Figure 5, B, C, and D). This damage progressed at d 3 postinstillation in the 1-mg group only (Figure 5, E and F). By d 6 postinstillation, there were minimal to no changes noted in any of the treatment groups (data not shown); however, TiO_2 particulate was still observed to be present in the lungs of rats exposed to the high dose (data not shown).

To assess lung injury, LDH activity, an indicator of general cytotoxicity, and albumin, an indicator of a compromise in the gas–blood barrier, were measured in the acellular lavage fluid recovered from the lungs of the animals treated with the TiO_2 nanorod suspensions (Figure 6). LDH activity

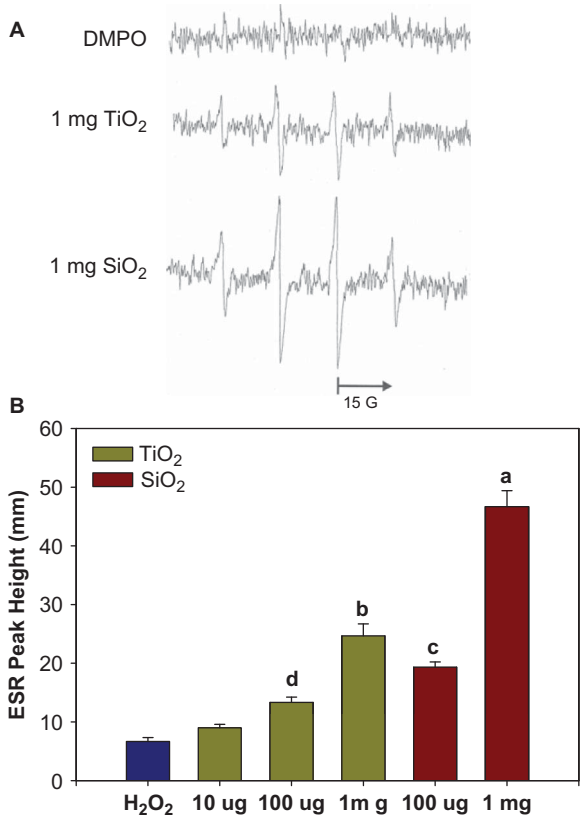

FIGURE 3. Particle free radical intermediates. Electron spin resonance (ESR) was performed on the TiO_2 nanorods at doses of 1 mg, 100 μg, and 10 μg in the presence of H_2O_2 and the spin trap, DMPO, to assess hydroxyl radical formation as an indicator of particle reactivity. Silica α-quartz (SiO_2) at doses of 1 mg and 100 μg was used as the positive control for the presence of the hydroxyl radical signal in a particle. Three analyses were performed for each sample. (A) Representative ESR spectra of the particles analyzed. (B) Quantification of the height of the peak relative to control (H_2O_2) as an indicator of the relative amount of hydroxyl radical formed. a, b, c, Significantly different from other groups; d, significantly different from 1 mg SiO_2, 100 μg SiO_2, 1 mg TiO_2, and H_2O_2; values are means ± standard error ($p < .05$) (color figure available online).

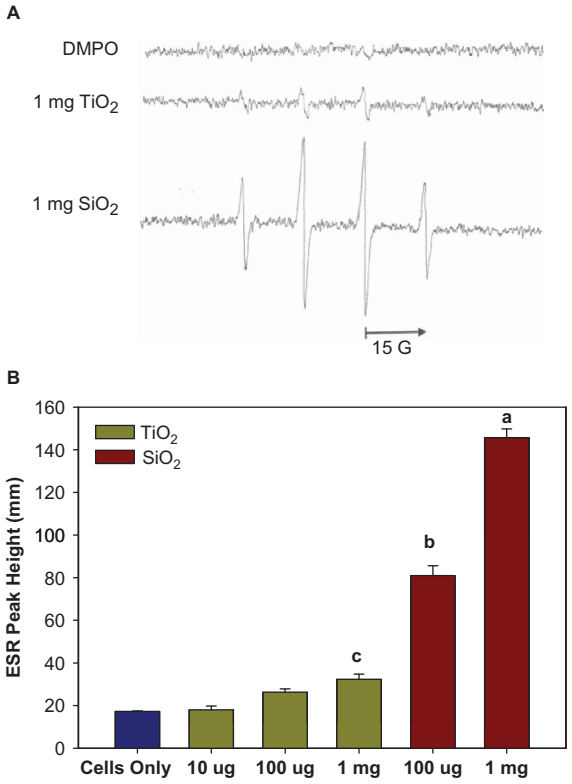

FIGURE 4. In vitro production of free radicals. Electron spin resonance (ESR) was performed on macrophages recovered from naïve rats. Cells were treated with 1 mg, 100 μg, or 10 μg TiO_2 in the presence of the spin trap, DMPO, to assess hydroxyl radical formation. Silica α-quartz (SiO_2) at doses of 1 mg and 100 μg was used as a positive control for the presence of the hydroxyl radical signal. Three analyses were performed for each treatment. (A) Representative ESR spectra of the cells treated with 1 mg TiO_2 or 1 mg SiO_2. (B) Quantification of the height of the hydroxyl radical peak relative to control (cells only) as an indicator of the relative amount of hydroxyl radical formed. a, b, Significantly different from other groups; c, significantly different from 1 mg SiO_2, 100 μg SiO_2, and cells only; values are means ± standard error ($p < .05$) (color figure available online).

was significantly elevated in the 1-mg TiO_2 group at d 1 and 3 postinstillation, when compared to control (Figure 6A). At 1 and 3 d postinstillation, there was a significant rise in lavage fluid albumin in response to the highest dose of TiO_2 (Figure 6B). There were no significant differences between saline and TiO_2 groups at d 6. When comparing silica (positive control) to TiO_2 nanorods, there were no marked differences in LDH activity and albumin at any of the time points at each of the concentrations except for the 1-mg dose group at d 6, indicating persistence of the lung response after silica treatment but a resolution of the response for TiO_2.

To assess lung inflammation and immune responses, neutrophils, AM, and lymphocytes were recovered by whole lung lavage after treatment with the TiO_2 nanorod suspensions (Figure 7). The only significant differences observed in AM numbers among the TiO_2 group compared to control occurred on d 3, whereas AM number was significantly elevated in the 1-mg silica group on d 3 and 6 (Figure 7A). There was a dose-dependent

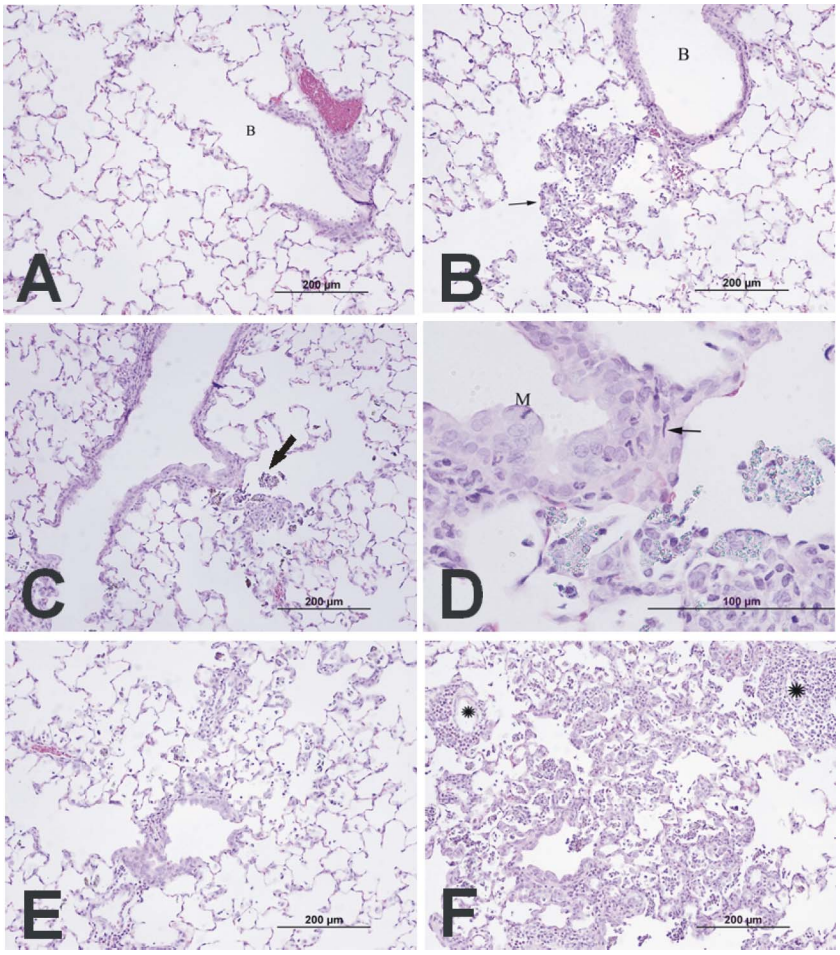

FIGURE 5. Histological analysis of H&E-stained tissue sections. Inflammation and lung injury were noted in the 1-mg and 100-µg groups 1 d post-instillation, and these persisted at d 3 post-instillation in the 1-mg group only. By d 6 post-instillation, despite the persistence of TiO_2 in the lungs, there were minimal changes noted in any of the treatment groups. (A) Saline group, 1 d post-instillation (10× objective). The terminal bronchiole (B) is lined by cuboidal epithelium. Very few cells are present in alveoli. (B) 100-µg TiO_2 group 1, d post-instillation (10× objective). The bronchiole (B) has a minimal infiltration of granulocytes in the submucosa. At the lower left is a terminal bronchiole with minimal degenerative changes in the epithelium (arrow), as well as some local infiltration of macrophages and a few granulocytes. (C) 1-mg TiO_2 group, 1 d post-instillation (10× objective). The bronchiole shows slightly thickened walls due to infiltration of granulocytes. Peribronchiolar inflammation is present at the lower center portion of the image. Dark refractile pigment (TiO_2) is surrounded by macrophages (arrow). (D) 1 mg TiO_2 group, 1 d post-instillation (40× objective). High-magnification photomicrograph of bronchiolar inflammation shows a few granulocytes migrating through the mucosa (arrow), as well as a mitotic figure (M) in the epithelium. Dark refractile pigment is surrounded and engulfed by macrophages. (E) 1-mg TiO_2 group, 3 d post-instillation (10× objective). Terminal bronchiole has mild regenerative changes (increased cytoplasmic basophilia) in the epithelium, and is surrounded by alveoli with thickened septa and that contain macrophages, pigment, and granulocytes. (F) 1-mg TiO_2 group, 3 d post-instillation (10× objective). Inflammation is moderate in this area, and is characterized by perivascular infiltration of leukocytes (lymphocytes and granulocytes, asterisk), as well as prominent alveolar septal thickening and alveolar pigment, macrophages, and a few granulocytes (color figure available online).

increase in neutrophils 1 d postinstillation of TiO_2 or silica when compared to control rats (Figure 7B). Lung neutrophil number remained elevated in only the 1-mg TiO_2 and silica groups throughout the 6-d postinstillation period compared to control. A significant elevation in neutrophil number was observed with 1 mg silica at d 6 compared to TiO_2. Lymphocyte numbers were significantly elevated in the 100-µg and 1-mg silica groups when compared to controls and all TiO_2 groups 1 d postinstillation (Figure 7C). Lymphocytes

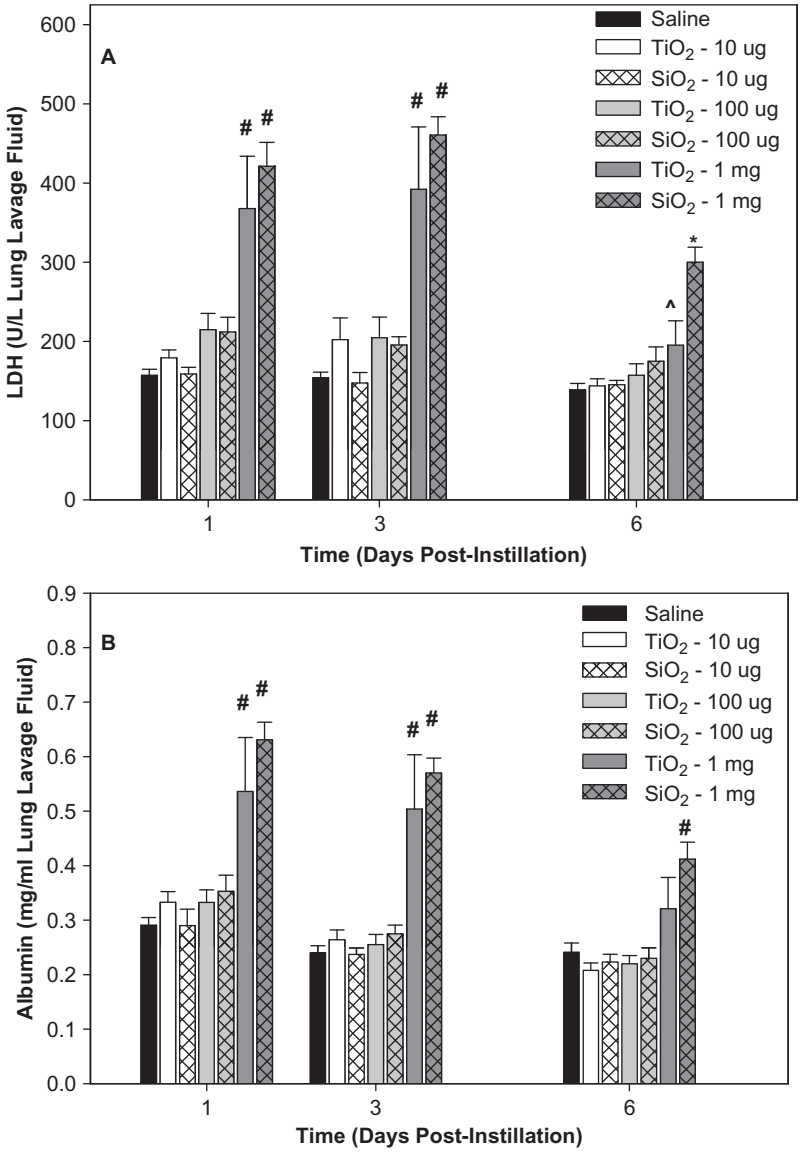

FIGURE 6. Indices of lung injury measured in the first fraction of lung lavage fluid at 1, 3, and 6 d after intractracheal instillation with 1 mg, 100 μg, or 10 μg of TiO_2 nanorods, silica α-quartz (SiO_2), or saline: (A) Lactate dehydrogenase (LDH) and (B) albumin. Asterisk indicates significantly different from all groups within a time point; #, significantly different from saline, TiO_2 10 μg, SiO_2 10 μg, TiO_2 100 μg, and SiO_2 100 μg within a time point; ^, significantly different from saline, TiO_2 10 μg, and SiO_2 10 μg within a time point; values are means ± standard error ($n = 8$–14 saline, $n = 8$ TiO_2, $n = 6$ SiO_2; $p < .05$).

remained significantly elevated in the high-dose silica group when compared to all groups throughout the time course. In, addition, by d 6, there were still significant increases in lymphocyte number in the lower doses of silica when compared to equal doses of TiO_2 or control.

With regard to uptake of particles by AM, transmission electron microscopy showed that the TiO_2 nanorods were readily engulfed by AM (Figure 8, A and B). Individual nanorods in AM were analyzed using EDX analysis to confirm that the particles imaged were TiO_2 nanorods (Figure 8, C and D). The particles were observed in AM at all time points in all doses after instillation (data not shown).

Numerous cytokines and chemokines related to the inflammatory pathway and

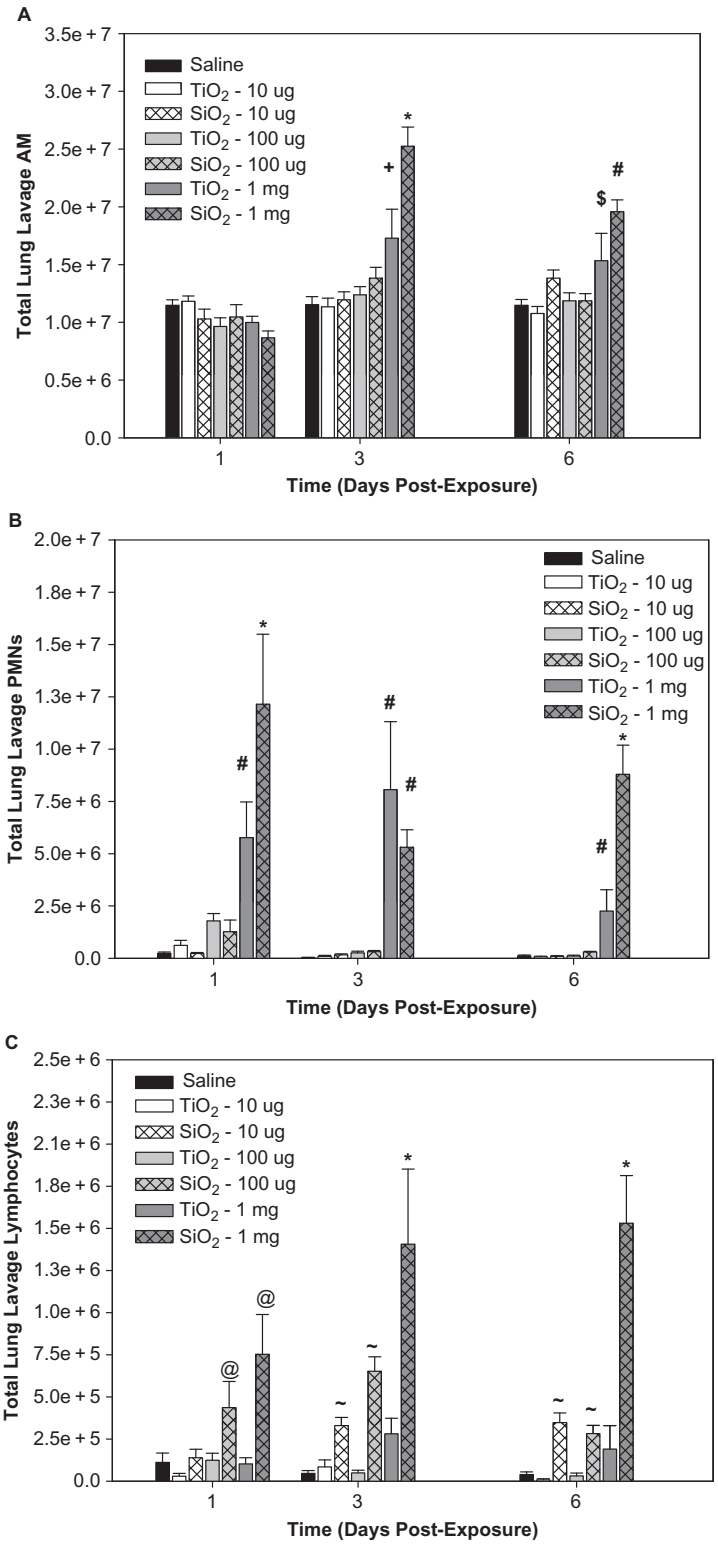

FIGURE 7. Total number of (A) alveolar macrophages (AM), (B) neutrophils (PMNs), and (C) lymphocytes recovered in lung lavage fluid from rats 1, 3, and 6 d after intratracheal instillation with 10 μg, 100 μg, 1 mg of TiO_2 nanorods, silica α-quartz (SiO_2) or saline. Asterisk indicates significantly different from all groups within a time point; #, significantly different from saline, TiO_2 10 μg, SiO_2 10 μg, $TiO_2$100 μg, and $SiO_2$100 μg within a time point; $^+$, significantly different from saline, TiO_2 10 μg, SiO_2 10 μg, and TiO_2 100 μg within a time point; $, significantly different from saline, TiO_2 10 μg, TiO_2 100 μg, and SiO_2 100 μg within a time point; @, significantly different from saline, TiO_2 10 μg, SiO_2 10 μg, $TiO_2$100 μg, and TiO_2 1 mg within a time point; ∼, significantly different from saline, TiO_2 10 μg, and TiO_2 100 μg within a time point; values are means ± standard error (n = 8–14 saline, n = 8 TiO_2, n = 6 SiO_2; $p < .05$).

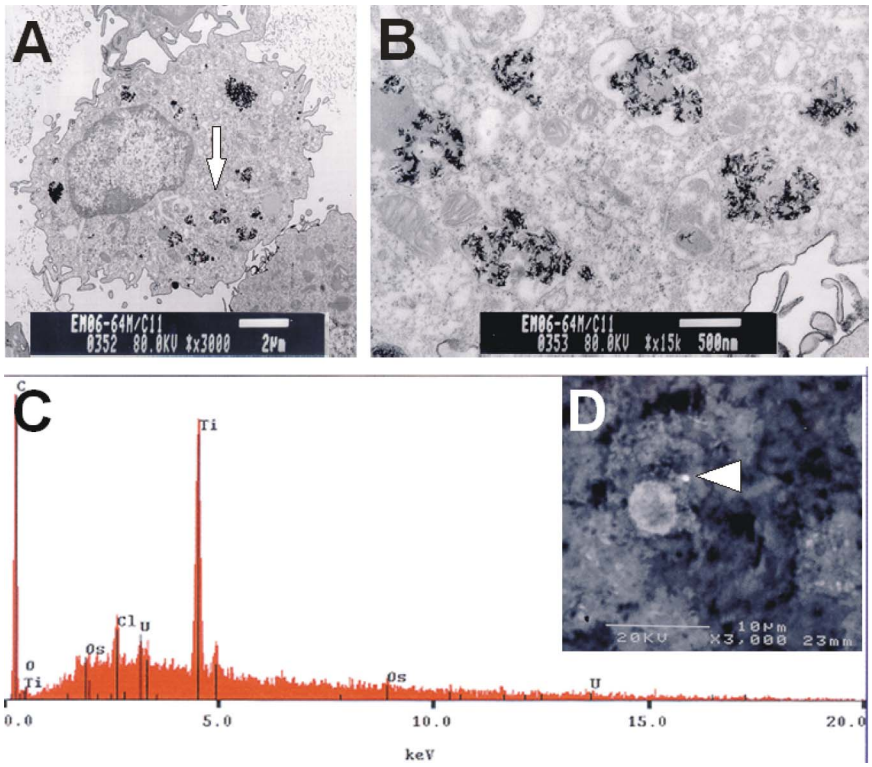

FIGURE 8. Alveolar macrophage uptake of TiO_2. (A) Transmission electron microscopy (TEM) image of an AM from a rat 1 d after instillation with 100 μg TiO_2 showing phagocytosis of the particles (arrow) (B) High-magnification TEM image of area indicated by arrow in (A). (C) Elemental spectra of an AM vacuole containing nanorods analyzed using energy dispersive x-ray (EDX) analysis at 20 kV to confirm that the particles imaged were TiO_2. (D) Scanning electron microscopy (SEM) backscatter image corresponding to (C). The arrowhead indicates the vacuole in the AM that underwent elemental mapping. The particles were observed in AM at all time points in all doses post-instillation (data not shown) (color figure available online).

immune function were measured in the acellular lung lavage fluid after treatment with the TiO_2 nanorods or silica (Figure 9). There were no significant differences in TNF-α although there was trend for a rise in all silica groups relative to TiO_2 groups (Figure 9A). There was a significant increase in IL-12p70 in all silica-treated rats relative to TiO_2-treated rats on d 1 and a significant decrease was observed in all silica-treated animals on d 3 relative to the TiO_2 groups (Figure 9B). No significant differences were observed when comparing levels of IL-10, an anti-inflammatory cytokine that inhibits macrophage function, among TiO_2-treated rats relative to saline controls. However, this cytokine was diminished significantly in silica-treated rats at all time points postexposure relative to saline controls and TiO_2-treated rats (Figure 9C), indicative of a release of inhibition on macrophages. There were significant increases in chemokines, MCP-1 and MIP-2, measured in TiO_2-treated rats at the high dose. MCP-1 was significantly elevated on d 1 and 3 postinstillation in the rats treated with 1 mg of TiO_2 nanorods relative to the saline group; however, there were no significant differences between increases observed when comparing the rats treated with TiO_2 nanorods versus rats treated with silica at the equivalent doses (data not shown). MIP-2 was significantly elevated on d 1 postinstillation in the rats treated with 1 mg of TiO_2 nanorods compared to saline controls and rats treated with 10 μg of TiO_2 nanorods or silica (Figure 9D); however, the rise was nearly fivefold greater in rats treated with 1 mg silica. In addition, rats treated with 100 μg or 1 mg silica also showed significantly elevated

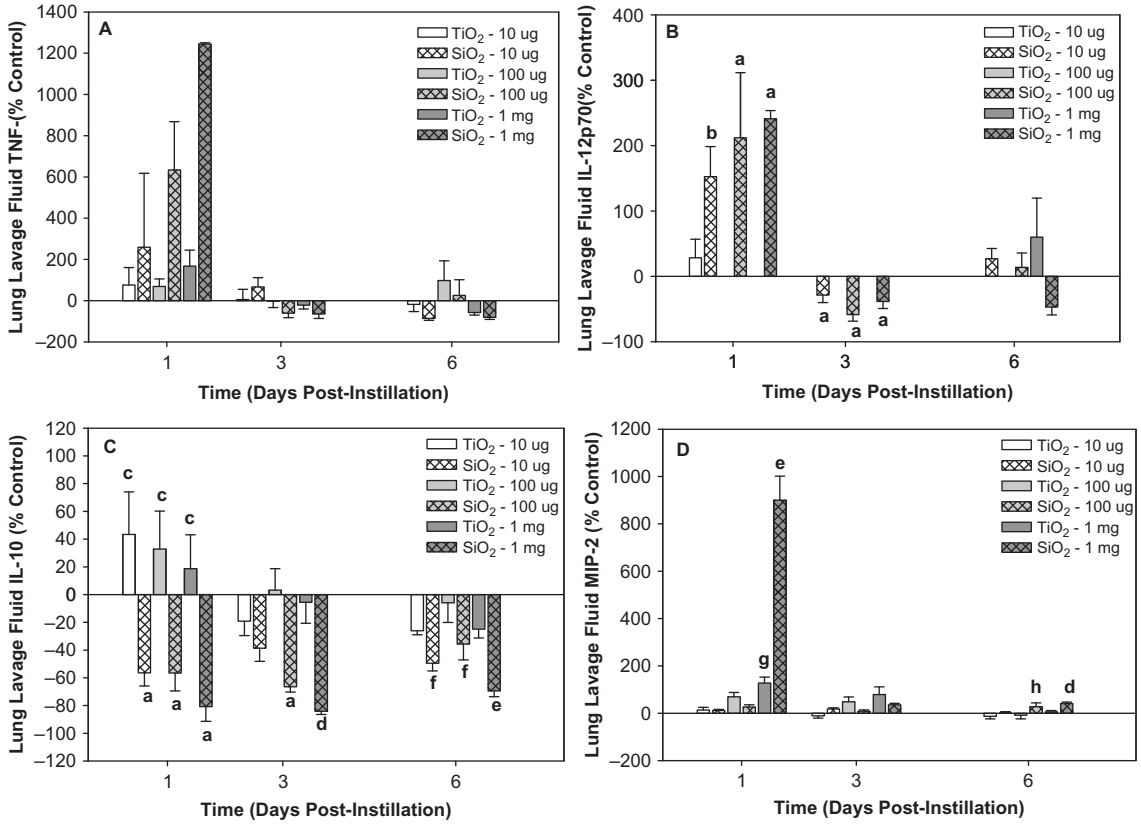

FIGURE 9. Inflammatory cytokines, (A) TNF-α (B) IL-12p70, anti-inflammatory cytokine (C) IL-10, and chemokine, (D) MIP-2, in the first fraction of lung lavage fluid recovered from rats intratracheally instilled with 1 mg, 100 μg, or 10 μg TiO_2 nanorods, silica α-quartz (SiO_2), or saline 1, 3, or 6 d post-instillation. Mean control value ranges across timepoints (pg/ml lung lavage fluid): TNF-α= 5.21–10.98, IL-12p70 = 8.52–23.47, IL-10 = 129.4–193.9, MIP-2 = 405.2–478.0. a, significantly different from TiO_2 10 μg, TiO_2 100 μg, and TiO_2 1 mg within a time point; b, significantly different from TiO_2 100 μg and TiO_2 1 mg within a time point; c, significantly different from SiO_2 10 μg, SiO_2 100 μg, and SiO_2 1 mg within a time point; d, significantly different from TiO_2 10 μg, SiO_2 10 μg, TiO_2 100 μg, and $TiO_2$1 mg within a time point; e, significantly different from all groups within a time point; f, significantly different from TiO_2 100 μg within a time point; g, significantly different from TiO_2 10 μg and Si 10 μg within a time point; h, significantly different from TiO_2 10 μg and TiO_2 100 μg within a time point; values are means $\pm$ standard error (n = 8–14 saline, n = 8 TiO_2; n = 6 SiO_2; $p < .05$).

levels of MIP-2 in the lung lavage fluid on d 6 postexposure compared to rats treated with TiO_2 nanorods. These increases in MCP-1 and MIP-2 correspond well with cellular influx of AM and neutrophils into the lungs of rats in these treatments group. There were no significant differences observed in the acute phase cytokine, IL-6, and immune cytokines, IL-2, IL-4, or IFN-γ, in the lung lavage fluid among TiO_2 nanorod treatment groups at any time point (data not shown).

To assess the immune effect of TiO_2 nanorods on defense responses to bacterial challenge, animals were treated on d 0 with 100 μg or 1 mg of TiO_2 nanorods, the lungs of the treated animals were inoculated with *Listeria monocytogenes* on d 3 after TiO_2 treatment, and bacterial clearance was determined on d 6, 8, and 10 (Figure 10). There was no significant difference in morbidity, animal body weight change (data not shown), and the clearance of *L. monocytogenes* after pretreatment with either dose of TiO_2 nanorods compared to control.

DISCUSSION

One goal of this study was to characterize and assess pulmonary responses after exposure to a non-dispersed TiO_2 nanorod. A sample of the TiO_2 nanorods was suspended in PBS and intratracheally instilled

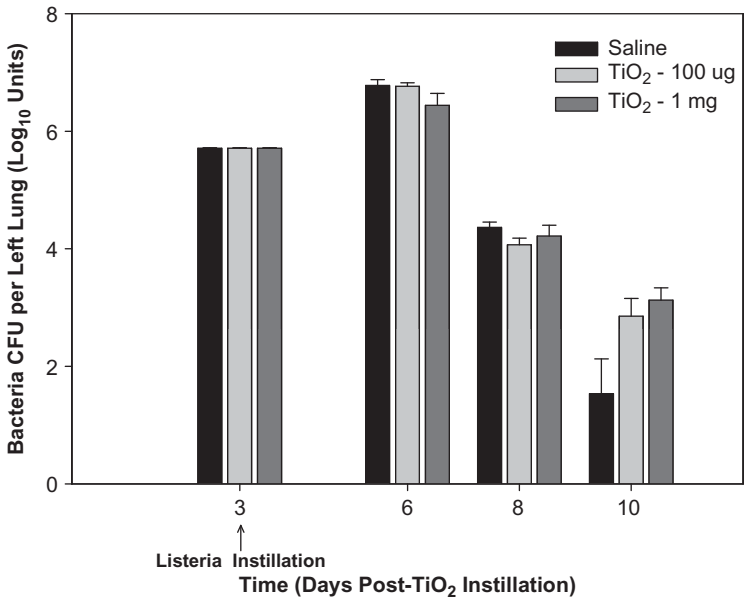

FIGURE 10. Number of bacterial colony-forming units (CFUs) in the left lungs of rats that were preexposed to 100 μg TiO_2 nanorods, 1 mg Ti nanorods, or saline 3 d prior to intratracheal inoculation with 5×10^5 *L. monocytogenes*. Values are means ± standard error (n = 6/treatment group/time point).

into the lungs of animals. Particle agglomeration of the nanorod suspension was examined, and x-ray scattering and electron microscopy showed primary particle clusters of 3–4 rods oriented along their length and arranged in complex agglomerates in suspension with an average particle diameter in the range of 500–2800 nm. The level of agglomeration observed with the suspended TiO_2 nanorods was not surprising. Particle agglomeration may be an important obstacle in examining the pulmonary toxicity of nanomaterials. The suspension of nanoparticles in other media, such as lung lavage fluid or PBS that contained proteins plus a phospholipid (dipalmitoyl phosphatidylcholine), was observed to improve particle dispersion and reduce agglomeration (Sager et al. 2007). However, the addition of exogenous proteins and phospholipids to the suspension medium may coat the nanomaterials and attenuate or alter the surface reactivity, toxicity, and/or time frame of adverse responses of the particles (Gao et al. 2000). Thus, for the initial experiments for the current study, the response of non-dispersed TiO_2 nanorods, suspended in untreated PBS, was examined. In a separate study, the analysis of pulmonary toxicity of dispersed TiO_2 nanorod is ongoing.

Studies have shown that evaluating the surface reactivity of nanoparticles in cell-free and cell-based systems provide a potential predictor of acute pulmonary toxicity *in vivo* (Rushton et al. 2010). Previous pulmonary bioassay studies using poorly dispersed nanoparticles indicated that particle surface reactivity and not primary particle size or surface area correlated best with inflammatory potential after treatment with different sized silica (α-quartz) and TiO_2 particles (Warheit et al. 2006; 2007c; 2009). For the current study, ESR was performed on suspensions of TiO_2 nanorods and silica, both cell-free and in the presence of AM, to determine particle surface bioreactivity. ESR analysis showed silica particles to be highly reactive and generate significant levels of ROS on the particle surface (Vallyathan et al. 1988). In both the cell-free and cell-based assays, the TiO_2 nanorods generated a concentration-dependent increase in hydroxyl radicals that was statistically greater than control values at the highest concentrations but significantly less than hydroxyl generation produced by silica treatment.

In agreement, Reeves et al. (2008) observed TiO_2 nanoparticles to increase hydroxyl radical formation in a cellular in vitro

assay as measured by ESR. Hamilton et al. (2009) demonstrated that both short (<5 μm) and long (>15 μm) TiO_2 nanobelts elevated intracellular ROS production and lipid peroxidation. A rise in ROS generation may be one mechanism by which inhaled nanoparticles may be cytotoxic to pulmonary cells. This may be especially important for nanomaterials in that as particle size is reduced, the proportion of atoms associated with the surface is magnified relative to the proportion inside its volume, possibly generating more reactive particles (Warheit et al. 2009). If the ESR results of the current study are normalized to surface area for a given mass of silica versus TiO_2 nanorods, the surface area of the nanorods would be greater than that of the fine-sized silica; however, the silica particle reactivity at equivalent mass is approximately 2 time greater in the cell free system, and 5–6 times greater in the in vitro ESR system. Overall, when compared to the highly reactive, highly toxic silica particles, the TiO_2 nanorods used in this study are significantly less reactive; nonetheless, the TiO_2 nanorods did have significant surface reactivity compared to control. Based on these ESR findings of an elevation in hydroxyl radical by the TiO_2 nanorod suspension used in the current study, it would seem possible that this particular nanomaterial at high concentration may produce adverse responses in the lungs.

Histopathology and lung lavage fluid analysis revealed minimal changes in lung injury and inflammation early after i.t. instillation with 10 or 100 μg of TiO_2 nanorods. These responses quickly subsided and were no different from control values by 3 d after treatment. Pulmonary inflammation and injury were more significant and still elevated at 3 d after treatment with 1 mg of TiO_2 nanorods, but by 6 d, lungs appeared normal even at this higher TiO_2 dose. Because these responses subsided by 6 d after treatment, it is highly doubtful that this particular TiO_2 nanorod possesses fibrogenic properties, unlike other fiber-shaped nanomaterial, such as carbon nanotubes (Shvedova et al. 2005). At a comparable dose of 1.2 mg of TiO_2 particles with a mean diameter of 0.9 μm, Rehn et al. (2003) observed a similar elevation in lung inflammation and lung lavage fluid injury parameters at 3 d that quickly resolved over time. The 10-μg, 100-μg, and 1-mg TiO_2 doses used in the current study correspond to 0.03 mg/kg, 0.33 mg/kg, and 3.3 mg/kg, respectively. Comparable results were observed in other lung rat toxicity studies that used 1-mg/kg and 5-mg/kg doses of TiO_2 nanorods. Transient and reversible increases in lung inflammation and some lung lavage fluid biochemical injury parameters were observed for both doses of TiO_2 nanorods at 1 d after exposure (Nemmar et al. 2008; Warheit et al. 2006). In contrast, well-dispersed TiO_2 nanospheres (0.26 mg/rat) were reported to induce substantial lung inflammation, which remained well above control at 42 d postexposure (Sager et a. 2008).

Electron microscopy revealed that significant portions of deposited TiO_2 nanorods were phagocytized by AM after IT instillation and still present in the cells at all time points examined after treatment. In the characterization of AM/TiO_2 nanoparticle interaction, Hamilton et al. (2009) demonstrated that TiO_2 nanospheres and short nanobelts (< 5 μm) were taken up in the cytoplasm in discrete lysosomes in the cell, similar to what was observed with TiO_2 nanorods in the current study. In contrast, AM exposed to long nanobelts (>15 mm) failed to produce functional lysosomes, resulting in the subsequent release of cathepsin B and the formation of NALP3 inflammasome. This dysfunction of AM-particle processing was observed with asbestos and silica, and appears unlikely to occur after exposure to shorter length TiO_2 nanorods, such as those used in this study.

AM are a critical part of lung defense mechanisms in response to bacterial infection, with a direct bactericidal role, as well as producing bactericidal oxidants and cell signaling molecules involved in innate and adaptive immune responses. Despite the increased burden of TiO_2 nanorods in AM used in the current study, there appears to be no marked effect on lung defense functions after exposure. AM exposed to TiO_2 nanorod samples in vitro were able to generate oxidants as measured

by ESR. In addition, inflammatory cytokines and chemokines produced by AM, as well as neutrophils, were elevated in the lung lavage fluid of rats exposed to TiO_2 nanorods in vivo, although to a lesser degree than those from rats treated with silica. No significant alterations in lung lavage fluid levels of cytokines related to adaptive immunity in the lung (IL-2, IL-4, IL-10, or IFN-γ) were observed in rats treated with TiO_2 nanorods when compared with controls. In addition, immune responses of TiO_2 nanorod-treated rats after challenge with a bacterial pathogen were not markedly altered, indicating the response of macrophages in the killing and clearing of bacteria from the lungs was not markedly impaired. Pulmonary treatment with the two high doses of TiO_2 nanorods before inoculation with *L. monocytogenes* did not affect the ability of the lung to clear the bacteria. Previous studies by our group have indicated that other examples of nanoparticles, single-walled carbon nanotubes or welding fumes, suppress immune defense responses, possibly increasing the susceptibility of the lungs to infection (Antonini et al. 2007; Shvedova et al. 2008), and subchronic exposure to silica was shown to produce the opposite effect resulting in a faster clearance of the infection due to significantly heightened AM activation (Antonini et al. 2000a; 2000b).

Another goal of this study was to establish a well-characterized (in terms of size, shape, and surface properties) rod-shaped nanomaterial to be used as a control reference particle for the toxicological assessment of other nanorod/wire/fiber materials as part of the NIOSH nanotechnology research initiative (NIOSH 2009). From the results of this current study, this specific TiO_2 nanorod may be an appropriate candidate for use as a control reference particle, particularly at the lower doses, which may be more physiologically relevant in terms of worker exposure scenarios and better reflect the LOEL or NOEL. In the non-dispersed form, it produced no adverse effect on lung immune function after challenge with a bacterial pathogen and had a low inflammatory potential over a wide dose range. The elevations in lung injury and inflammation that were observed at the high dose 1 d after instillation were transient and reversible, and may be due to the method of administration to the animals. Intratracheal instillation introduces a large bolus of material in the lungs that may be responsible for the early elevations in inflammation observed after treatment (Driscoll et al. 2000); therefore, it may be more pertinent to examine the earliest inflammatory responses at 2 or 3 d after treatment to ensure the response is due to inherent properties of the nanomaterial and not to due to administration procedure. In addition, there is debate as to whether the dispersed or non-dispersed form of a nanomaterial is the more appropriate form to evaluate in terms of toxicity related to occupational exposure. Sager et al. (2007) demonstrated that pulmonary inflammation was 8-fold greater 1 d after IT instillation exposures to well-dispersed versus poorly-dispersed carbon black nanoparticles. In addition, concerning pulmonary exposures, agglomerates that reach the alveolar region may further disperse in or interact with the surfactant layer in the lung. Studies are currently underway to determine whether there is any variation in pulmonary toxicity when TiO_2 nanorods are administered to rats in a physiologically based dispersion medium.

REFERENCES

American Society for Testing and Materials. 2002. ASTM B922-02: Standard test method for metal powder specific surface area by physical adsorption. West Consohocken, PA: ASTM International.

Antonini, J. M., Yang, H.-M., Ma, J. Y. C., Roberts, J. R., Barger, M. W., Butterworth, L., Charron, T. G., and Castranova, V. 2000a. Subchronic silica exposure enhances respiratory defense mechanisms and the pulmonary clearance of *Listeria monocytogenes* in rats. *Inhal. Toxicol.* 12:1017–1036.

Antonini, J. M., Roberts, J. R., Yang, H-M., Barger, M. W., Ramsey, D., Castranova, V., and Ma, J. Y. C. 2000b. Effect of short-term silica inhalation on the pulmonary clearance of a bacterial pathogen in Fischer 344 rats. *Lung*. 178:341–350.

Antonini, J. M., Roberts, J. R., Jernigan, M. R., Yang, H-M., Ma, J. Y. C., and Clarke, R. W. 2002. Residual oil fly ash increases the susceptibility to infection and severely damages the lungs after pulmonary challenge with a bacterial pathogen. *Toxicol. Sci.* 70:110–119.

Antonini, J. M., Stone, S., Roberts, J. R., Chen, B., Schwegler-Berry, D., Afshari, A. A., and Frazer, D. 2007. Effect of short-term stainless steel welding fume inhalation exposure on lung inflammation, injury, and defense in rats. *Toxicol. Appl. Pharmacol.* 223: 234–245.

Brain, J. D., Knudson, D. E., Sorokin, S. P., and Davis, M. A. 1976. Pulmonary distribution of particles given by intratracheal instillation or by aerosol inhalation. *Environ. Res.* 11: 3–33.

Brown, D. M., Wilson, M. R., MacNee, W., Stone, V., and Donaldson, K. 2001. Size-dependent proinflammatory effects of ultrafine polystyrene particles: A role for surface area and oxidative stress in the enhanced activity of ultrafines. *Toxicol. Appl. Pharmacol.* 175:191–199.

Brown, J. S., Zeman, K. L., and Bennett, W. D. 2002.Ultrafine particle deposition and clearance in the healthy and obstructed lung. *Am. J. Respir. Crit. Care Med*.166:1240–1247.

Chen, X., and Mao, S. S. 2006. Synthesis of titanium dioxide (TiO_2) nanomaterials. *J. Nanosci. Nanotechnol*. 6:906–925.

Cohen, M. D., Sisco, M., Zelikoff, J. T., and Schlesinger, R. B. 2001. Ozone-induced modulation of cell-mediated immune responses in the lungs. *Toxicol. Appl. Pharmacol.* 171:71–84.

Dankovic, D., Kuempel, E., and Wheeler, M. 2007. An approach to risk assessment for TiO_2. *Inhal. Toxicol.* 19(suppl. 1): 205–212.

Driscoll, K. E., Costa, D. L., Hatch, G., Henderson, R., Oberdorster, G., Salem, H., and Schlesinger, R. B. 2000. Intratracheal instillation as an exposure technique for the evaluation of respiratory tract toxicity: uses and limitations. *Toxicol. Sci.* 55: 24–35.

Formo, E., Lee, E., Campbell, D., and Xia, Y. 2008. Functionalization of electrospun TiO_2 nanofibers with Pt nanoparticles and nanowires for catalytic applications. *Nano. Lett.*8:668–672.

Gao, N., Keane, M. J., Ong, T., and Wallace, W. E. 2000. Effects of simulated pulmonary surfactant on the cytotoxicity and DNA-damaging activity of respirable quartz and kaolin. *J. Toxicol. Eviron. Health. A.* 60: 153–167.

Hamilton, R. F., Wu, N., Porter, D., Buford, M., Wolfarth, M., and Holian, A. 2009. Particle length-dependent titanium dioxide nanomaterials toxicity and bioactivity. *Part. Fibre Toxicol.* 6:35.

ICRP. 1994. *Human respiratory tract model for radiological protection*. Oxford, England: Pergamon, Elsevier Science Ltd. International Commission on Radiological Protection Publication No. 66.

Janzen, E. G., and Blackburn, B. J.1968. Detection and identification of short-lived free radicals by an electron spin resonance trapping technique. *J. Am. Chem. Soc.* 90:5909–5910.

Jaques, P. A., and Kim, C. S. 2000. Measurement of total lung deposition of inhaled ultrafine particles in healthy men and women. *Inhal. Toxicol.* 12:715–731.

Merget, R., Bauer, T., Kupper, H. U., Philippou, S., Bauer, H. D., Breitstadt, R., and Bruening, T. 2002. Health hazards due to inhalation of amorphous silica. *Arch. Toxicol.* 75: 625–634.

National Institute for Occupational Safety and Health. 1996. Elements (ICP): Method 7300. In *NIOSH manual of analytical methods*, 4th ed., issue 2, U.S. Department of Health and Human Services, Publication No. 98-119. Washington, DC: NIOSH.

National Institute for Occupational Safety and Health. 2007. *Progress toward safe nanotechnology in the workplace: A report from the NIOSH Nanotechnology Research Center* [DHHS (NIOSH) publication no. 2007-123], a progress report on the status of nanotechnology research conducted by the NIOSH NTRC through

2006. http://www.cdc.gov/niosh/docs/2007-123/pdfs/2007-123.pdf

National Institute for Occupational Safety and Health. 2009. *Strategic plan for NIOSH nanotechnology research and guidance: Filling the knowledge gaps*. NIOSH publication no. 2010-105. www.cdc.gov/niosh/docs/2010-105/pdfs/2010-105.pdf

National Science and Technology Council. 2006. *Environmental, health, and safety needs for engineered nanoscale materials*. The National Nanotechnology Initiative. www.nano.gov

Nel, A., Xia, T., Madler, L., and Li, N. 2006. Toxic potential of materials at the nanolevel. *Science* 311:622–627.

Nemmar, A., Melghit, K., and Ali, B. H. 2008. The acute proinflammatory and prothrombic effects of pulmonary exposure to rutile TiO_2 nanorods in rats. *Exp. Biol. Med.* 233: 610–619.

Oberdörster, G., Ferin, J., Gelein, R., Soderholm, S. C., and Finkelstein, J. 1992. Role of the alveolar macrophage in lung injury—Studies with ultrafine particles. *Environ. Health Perspect.* 97: 193–199.

Reeves, J. F., Davies, S. J., Dodd, N. J. F., and Jha, A. N. 2008. Hydroxyl radicals (·OH) are associated with titanium dioxide (TiO_2) nanoparticle-induced cytotoxicity and oxidative damage in fish cells. *Mutat. Res.* 640:113–122.

Rehn, B., Seiler, F., Rehn, S., and Maier, M. 2003. Investigations on the inflammatory and genotoxic lung effects of two types of titanium dioxide: Untreated and surface treated. *Toxicol. Appl. Pharmacol.* 189: 84–95.

Roco, M. C., and Bainbridge, W. S., eds. 2003. *Converging technologies for improving human performance: Nanotechnology, biotechnology, information technology and cognitive science*. Boston: Kluwer Academic (Springer).

Roberts, J. R., Young, S.-H., Castranova, V., and Antonini, J. M. 2007. Soluble metals in residual oil fly ash alter innate and adaptive pulmonary immune responses to bacterial infection in rats. *Toxicol. Appl. Pharmacol.* 221:306–319.

Rushton, E. K., Jiang, J., Leonard, S. S., Eberly, S., Castranova, V., Biswas, P., Elder, A., Gelein, R., Finkelstein, J., and Oberdorster, G. 2010. Concept of assessing nanoparticle hazards considering nanoparticle dosemetric and chemical/biological response-metric. *J. Toxicol. Environ. Health*. 73:445–461.

Sager, T. M., Porter, D. W., Robinson, V. A., Lindsley, W. G., Schwegler-Berry, D. E., and Castranova, V. 2007. Improved method to disperse nanoparticles for in vitro and in vivo investigation of toxicity. *Nanotoxicology.* 1:118–129.

Sager, T. M., Kommineni, C., and Castranova, V. 2008. Pulmonary response to intratracheal instillation of ultrafine versus fine titanium dioxide: Role of particle surface area. *Particle Fibre Toxicol.* 5:17.

Shvedova, A. A., Kisin, E. R., Mercer, R., Murray, A. R., Johnson, V. J., Potapovich, A. I., Tyurina, Y. Y., Gorelik, O., Arepalli, S., Schwegler-Berry, D., Hubbs, A. F., Antonini, J., Evans, D. E., Ku, B. K., Ramsey, D., Maynard, A., Kagan, V. E., Castranova, V., and Baron, P. 2005. Unusual inflammatory and fibrogenic pulmonary responses to single-walled carbon nanotubes in mice. *Am. J. Physiol.* 289:L698–L708.

Shvedova, A. A., Fabisiak, J. P., Kisin, E. R., Murray, A. R., Roberts, J. R., Tyurina, Y. Y., Antonini, J. M., Feng, W. H., Kommineni, C., Reynolds, J., Barchowsky, A., Castranova, V., and Kagan, V. E. 2008. Sequential exposure to carbon nanotubes and bacteria enhances pulmonary inflammation and infectivity. *Am. J. Respir. Cell. Mol. Biol.* 38: 579–590.

Vallyathan, V., Shi, X., Dalal, N. S., Irr, W., and Castranova, V. 1988. Generation of free radicals from freshly fractured silica dust. *Am. Rev. Respir. Dis.* 138:1213–1219.

Van Loveren, H., Rombout, P. J., Wagenaar, S. S., Walvoort, H. C., and Vos, J. G. 1988. Effects of ozone on the defense to a respiratory *Listeria monocytogenes* infection in the rat. Suppression of macrophage function and cellular immunity and aggravation

of histopathology in lung and liver during infection. *Toxicol. Appl. Pharmacol.* 94: 374–393.

Warheit, D. B., Hansen, J. F., Yuen, I. S., Kelly, D. P., Snajdr, S. I., and Hartsky, M. A. 1997. Inhalation of high concentrations of low toxicity dusts in rats results in impaired pulmonary clearance mechanisms and persistent inflammation. *Toxicol. Appl. Pharmacol.* 145:10–22.

Warheit, D. B., Webb, T. R., Sayes, C. M., Colvin, V. L., and Reed, K, L. 2006. Pulmonary instillation studies with nanoscale TiO_2 rods and dots in rats: Toxicity is not dependent upon particle size or surface area. *Toxicol. Sci.* 91:227–236.

Warheit, D. B., Hoke, R. A., Finlat, C., Donner, E. M., Reed, K. L., and Sayes, C. M. 2007a. Development of a base set of toxicity tests using ultrafine TiO_2 particles as a component of nanoparicle risk assessment. *Toxciol. Lett.* 171:99–110.

Warheit, D. B., Webb, T. R., Reed, K. L., Frerichs, S., and Sayes, C. M. 2007b. Pulmonary toxicity studt in rats with three forms of ultrafine-TiO_2 particles: Differential responses related to surface properties. *Toxicology.* 230: 90–104.

Warheit, D. B., Webb, T. R., Colvin, V. L., Reed, K. L., and Sayes, C. M. 2007c. Pulmonary bioassay with nanoscale and fine-quartz particles in rats: Toxicity is not dependent upon particle size but on surface characteristics. *Toxicol. Sci.* 95:270–280.

Warheit, D. B., Reed, K. L., and Sayes, C. M. 2009. A role for surface reactivity in TiO_2 and quartz-related nanoparticle pulmonary toxicity. *Nanotoxicology.* 3: 181–187.

Watanabe, M., Okada, M., Kudo, Y., Tonori, Y., Niitsuya, M., Sato, T., Aizawa, Y., and Kotani, M. 2002. Differences in the effects of fibrous and particulate titanium dioxide on alveolar macrophages of Fischer 344 rats. *J. Toxicol. Environ. Health A* 65:1047–1060.